Highly Stable Red-Emitting $Sr_2Si_5N_8:Eu^{2+}$ Phosphor with a Hydrophobic Surface

Zhang, Bi; Wang, Jun Wei; Hao, Lu Yuan; Xu, Xin; Agathopoulos, Simeon; Yin, Liang Jun; Wang, Cheng Ming; Hintzen, Hubertus T.Bert

DOI
10.1111/jace.14560

Publication date
2017

Document Version
Final published version

Published in
Journal of the American Ceramic Society

Received: 19 March 2016 | Accepted: 30 August 2016

DOI: 10.1111/jace.14560

ORIGINAL ARTICLE

Journal of the American Ceramic Society

Highly stable red-emitting $Sr_2Si_5N_8:Eu^{2+}$ phosphor with a hydrophobic surface

B. Zhang[1] | J.-W. Wang[1] | L.-Y. Hao[1] | X. Xu[1] | S. Agathopoulos[2] | L.-J. Yin[3,4] | C.-M. Wang[1] | H. T. (Bert) Hintzen[4]

[1]Department of Materials Science and Engineering, Chinese Academy of Science Key Laboratory of Materials for Energy Conversion, University of Science and Technology of China, Hefei, Anhui, China

[2]Materials Science and Engineering Department, University of Ioannina, Ioannina, Greece

[3]School of Energy Science and Engineering, University of Electronic Science and Technology of China, Chengdu, China

[4]Luminescent Materials Research Group, Faculty of Applied Sciences, Delft University of Technology, Delft, the Netherlands

Correspondence
Xin Xu, Department of Materials Science and Engineering, Chinese Academy of Science Key Laboratory of Materials for Energy Conversion, University of Science and Technology of China, Hefei, Anhui, China.
Email: xuxin@ustc.edu.cn

Abstract

One of the biggest problems in white light-emitting diodes (WLEDs) is the moisture-induced degradation of phosphors. This paper proposes a simple and feasible surface modification method to solve it, whereby a hydrophobic surface layer is developed on the surface of the phosphors. The particular case of orange-red-emitting $Sr_2Si_5N_8:Eu^{2+}$ (SSN) phosphor was investigated. The mechanism to develop the hydrophobic layer involves hydrolysis and polymerization of tetraethylorthosilicate (TEOS) and polydimethylsiloxane (PDMS). The experimental results showed that the surface layer of SSN phosphor was successfully modified to a hydrophobic nanolayer (8 nm) of amorphous silicon dioxide that contains CH_3 groups in the surface. This hydrophobic surface layer gives the modified phosphor superior stability in high-pressure water steam conditions at 150°C.

KEYWORDS

coatings, heat treatment, hydrolysis, nitrides, optical materials/properties

1 | INTRODUCTION

Solid-state lighting technology based on light-emitting diodes (LEDs) attracts great attention due to its high brightness, low energy consumption, long lifetime, and high reliability.[1,2] The phosphor conversion method is often used for generating white light. In particular, the emission of LED chips is down-shifted into useful green, yellow, or red light by phosphors. The phosphors used in solid-state lighting technology must have proper photoluminescence (PL), high quantum efficiency, low thermal quenching, and high reliability.[3–8]

However, thermal- and moisture-induced luminescence degradation of phosphors occurs during conventional applications, significantly reducing the reliability and shortening the lifetime of white LEDs.[2,9] For instance, it is well-known that thiogallate ($SrGaS_4$:Eu) and sulfide (CaS:Eu and SrS:Eu) phosphors are unstable;[10,11] several silicate and aluminate phosphors also exhibit a similar problem, even (oxy)nitride phosphors, which are generally considered to be very stable, are moisture-sensitive, as well.[12]

Orange-red-emitting $Sr_2Si_5N_8:Eu^{2+}$ (SSN) phosphor has great potential in warm white or high color-rendering LEDs. A highly efficient orange-red phosphor with a high quenching temperature allows the color-rendering properties of white LEDs to be improved.[2,13–15] However, it features serious luminescence degradation that prevents its wide commercialization, although it has a much lower production cost than the popular red-emitting $CaAlSiN_3:Eu^{2+}$ phosphor.[16]

The origin of the degradation in SSN phosphors has been reported in several works.[8,17,18] Moreover, the mechanism of degradation and possible methods of improving their stability have been also widely studied.[2,9,12,19] In particular, the improvement of water resistance was attempted via surface modifications. For instance, it was found that the PL properties of europium-doped strontium aluminate nanoparticles were maintained by surface modification

reaction with pyrophosphoric acid or 3-allyl-2,4-pentanedione.[20,21] A layer of $MAl_2B_2O_7$ (M=Sr, Ca, Ba) formed on the surface of MAl_2O_4:Eu^{2+}, Dy^{3+} phosphors also improved water resistance.[22] Moreover, heterocyclic compounds, β-diketones and multicarboxylic acids were used to achieve coordination with the surface cations in Eu^{2+}-activated strontium aluminates and improve water resistance.[23] These methods improved water resistance at room temperature. However, there are actually no systematic studies on minimizing the moisture-induced degradation at high temperatures, which is considerably more severe than that at room temperature. Our group has produced BN-coated SSN phosphors,[24] which had good moisture-resistance stability at the beginning of sequential damp heat tests (85°C/85%); however, their stability was reduced dramatically after a certain period of time.

Moisture-induced degradation is caused by the hydrolysis of the host and/or the oxidation of the luminescent center. A suitable layer may effectively isolate a phosphor particle from moist air. However, most inorganic films (for instance, pyrophosphate, silicate, and aluminate) are hydrophilic materials due to the presence of surface hydroxyl groups (–OH), which can easily absorb water molecules. These water molecules destroy the inorganic layer or diffuse through the layer and lead to luminescence degradation. A thick film can slowdown the degradation rate but it also has a negative effect on emission intensity. Thus, a modified hydrophobic surface layer might improve moisture resistance.

Polymer-derived ceramics obtained from pyrolysis of silicon-containing polymer precursors have gained increasing interest recently.[25,26] The resultant ceramic materials consist of Si–C, Si–O, and Si–N units. They are a new class of amorphous materials derived from the parent structure of polysilazane and polysiloxane.[25,27,28] It was reported that nanoporous silicon oxynitridocarbide inorganic fibers possess super hydrophobicity due to the presence of -CH_3 groups at the surface.[29]

The present paper presents a feasible synthetic approach to coat SSN particles with a hydrophobic surface layer through hydrolysis and polymerization of tetraethylorthosilicate (TEOS) and polydimethylsiloxane (PDMS). The modification process is expected to take place easily and to lead to strong interfacial bonding because of the similarity between the oxidized Si–O bonds in the surface of SSN phosphors and the Si–O bonds in the hydrophobic surface layer.

2 | MATERIALS AND EXPERIMENTAL PROCEDURE

Fine powders of Eu_2O_3 (>99.9999%, Shenzhen Quanjin Trading Co., Shenzhen, China) and $SrCO_3$ (AR, Guoyao Chemical Reagent Co., Shanghai, China) were dissolved in nitric acid with the composition of $Sr_{1.95}Eu_{0.05}Si_5N_8$. To this nitrate solution, ethanol solution that contained a stoichiometric amount of TEOS (AR, Guoyao Chemical Reagent Co.) was added, followed by the addition of an appropriate amount of citric acid. The solution was heated at ~80°C under continuous stirring with the aid of a magnetic agitator. After several hours, a transparent sol was formed. Further heating under constant stirring allowed the transformation of the sol to a transparent sticky gel. The gel was calcined at 600°C for 4 hour; the obtained product was milled and sieved. The resultant material was placed in a BN crucible, which was placed in an alumina tubular furnace. Firing took place at 1400°C for 4 hour under a flowing gas mixture of NH_3 and CH_4 (1.0 vol%). Cooling took place naturally inside the furnace under flowing NH_3 gas. Pure SSN phosphor powder was obtained.

To produce the hydrophobic surface layer, 0.625 g of the SSN phosphor was put into a 100 mL beaker, which contained a solution of 25 mL of heptane, 3 mL of PDMS (100 cSt, Acros, Geel, Belgium), and 1 mL of TEOS. Then, 10 drops of dibutyltindilaurate (DBTL, CP, Guoyao Chemical Reagent Co.) were added, which catalyzes the hydrolysis and condensation of TEOS. The mixture was stirred for 30 min. Then, 5 wt% of azodiisobutyronitrile (AIBN, AR. Tianjin Guangfu Fine Chemical Research Institute, Tianjin, China) was added, which acts as an initiator for PDMS polymerization, and the mixture was transferred into a spherical flask to reflux for 4 hour at 85°C. Followed by filtration under vacuum, the phosphor was washed with heptane and ethanol. At last, the SSN phosphor powder with surface modification (denoted as HB-SSN) was obtained after air drying for 24 hour.

The moisture-induced degradation test was carried out in an autoclave with Teflon lining,[12] as shown in Figure 1. About 0.2 g of SSN was put into a BN container, which was placed in a 50 mL autoclave. Then, 5 mL of water was added to the autoclave in such a way that the BN container was immersed in the water, but the phosphor inside the container did not make direct contact with the water. The autoclave was sealed and placed in an oven at a constant temperature for a certain time (48 hour). After the experiment, the sample was allowed to cool down to room temperature naturally inside the furnace and then dried at 100°C overnight.

The crystalline phases were identified by X-ray powder diffraction analysis (XRD, Philips PW 1700, Almelo, the Netherlands; $Cu_{K\alpha 1}$ radiation, λ = 1.54056 Å). The PL spectra were recorded at room temperature with a fluorescent spectrophotometer (F-4600, Hitachi, Tokyo, Japan, with a 200 W Xe lamp as an excitation source). The decay times were recorded with an FLS920 spectrophotometer (Edinburgh Instruments, Edinburgh, England). The microstructure of the powders was observed with a

scanning electron microscope (JEOL JSM-6390, equipped with a field-emission gun at an acceleration voltage of 20.0 kV, Tokyo, Japan). Their structure was also investigated by high-resolution transmission electron microscopy (ARM-200F, Tokyo, Japan). Fourier transform infrared spectroscopy (FT-IR) was carried out in a Perkin-Elmer 580B IR spectrophotometer with the KBr pellet technique (Waltham, MA). The X-ray absorption spectra for the Eu L_{III}-edge were measured at a beam line of BL14W1 at the Shanghai Synchrotron Radiation Facility. Thermal analysis (DTA/DGA) was done in air atmosphere with a Shimadzu DTG-60H thermobalance (Kyoto, Japan) at temperatures of up to 1000°C with a heating rate of 10 K/min.

3 | RESULT AND DISCUSSION

The influence of temperature on the PL spectra and the intensity at the emission maximum of SSN and HB-SSN treated in a moist atmosphere for 48 h is shown in Figure 2(A). A single emission band was recorded in all cases under excitation at 365 nm in the region of 550–800 nm. The emission intensity of the SSN phosphor degrades dramatically for temperatures higher than 120°C and the luminescence loss is nearly 45% at 150°C, whereas HB-SSN maintains 91% of the initial intensity (i.e., before the moisture test). It is also noteworthy that surface modification did not jeopardize the emission behavior and intensity. The emission intensity SSN was enhanced by 2% of the initial intensity. Accordingly, surface modification can effectively improve the moisture resistance from the fact that the emission intensity of the SSN is less than 54% of the HB-SSN after the moisture test at 150°C. The slight decrease in the emission intensity of HB-SSN at temperatures higher than 120°C might be partially attributed to agglomerations formed during the moisture test. This emission decrease caused by particle agglomerations is also observed in other phosphors.[30]

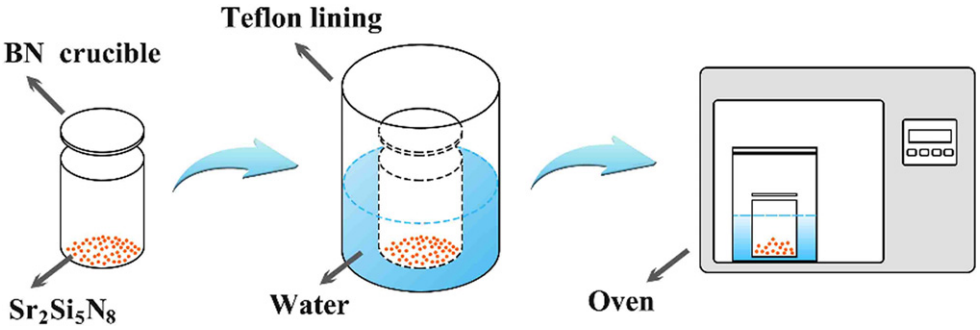

FIGURE 1 Moisture-induced degradation experiment [Color figure can be viewed at wileyonlinelibrary.com]

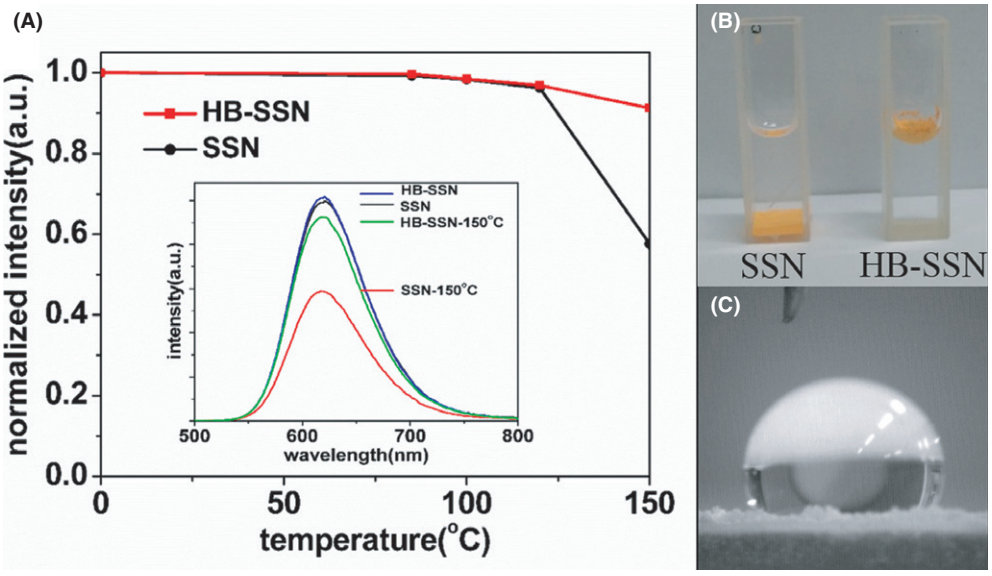

FIGURE 2 A, Emission intensity excited at 425 nm of SSN and HB-SSN treated with water steam at different temperatures for 48 hour (the inset shows the photoluminescence spectra); B, photographs of SSN and HB-SSN powders in water; C, contact angle of water drop on the surface of HB-SSN (at room temperature) [Color figure can be viewed at wileyonlinelibrary.com]

The surface of HB-SSN had clear hydrophobic properties with PDMS mixed with SiO_2, because the SSN particles sink to the bottom of the container in the water, whereas the HB-SSN particles do not sink to the bottom of the container (Figure 2B), and because a contact angle of ~110° (ie, a poor wetting regime) was formed between the surface of a pressed HB-SSN cake and water (at room temperature) (Figure 2C). Meanwhile, contact angle measurement of SSN is impossible, because it is totally hydrophilic, so the water droplet will permeate through the phosphor powder immediately.

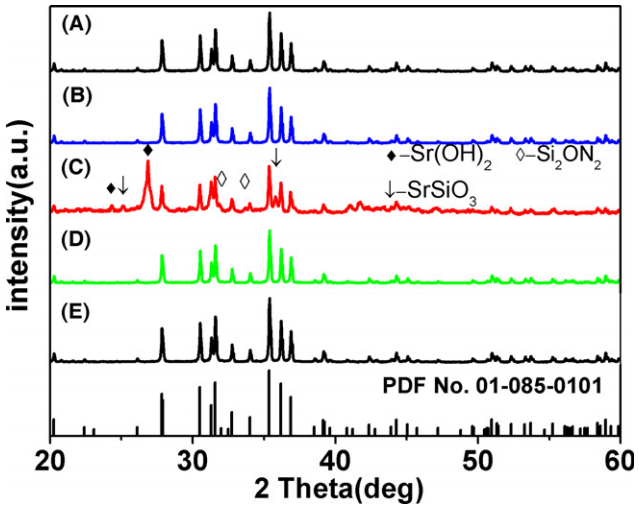

FIGURE 3 X-ray diffractograms of SSN (A: as-prepared, B: treated at 120°C, C: treated at 150°C), and HB-SSN (D: as-prepared, E: treated at 150°C). The diffraction patters SSN (JCPD No. 36-0570) are also plotted [Color figure can be viewed at wileyonlinelibrary.com]

The X-ray diffractograms of SSN and HB-SSN before and after the moisture tests, shown in Figure 3, suggest that both of these phosphors feature high purity and crystallinity. The surface-modified HB-SSN showed a remarkable stability after the treatment at 150°C, which could be attributed to the hydrolysis resistance from the hydrophobic groups. The samples of SSN remain stable after treatment up to 120°C for 48 hour. However, new phases of $SrSiO_3$, Si_2ON_2, and $Sr(OH)_2$ developed after treatment at 150°C, can be attributed to hydrolysis of $Sr_2Si_5N_8$ with the participation of H_2O and O_2:

$$Sr_2Si_5N_8 \xrightarrow{H_2O,O_2} SrSiO_3, Sr(OH)_2, Si_2ON_2, NH_3 \quad (1)$$

Moreover, an irritant smell occurred after the experiment (SSN, 150°C, 48 hour) and many small crystals of NH_4HCO_3 (indentified by XRD) were observed in the inner surface of the BN lid:

$$NH_3 + CO_2 + H_2O \longrightarrow NH_4HCO_3 \quad (2)$$

These findings agree fairly well with the conclusions drawn from the above analysis of the PL behavior (Figure 2A).

Microstructure observations of Figure 4 agree with the above results. Both the SSN and HB-SSN powders have prismatic particles with well-formed edges, which suggest high crystallinity and smooth surfaces. After treatment at 150°C, the particles of HB-SSN maintain their initial shape, whereas many small particles appear in the SSN

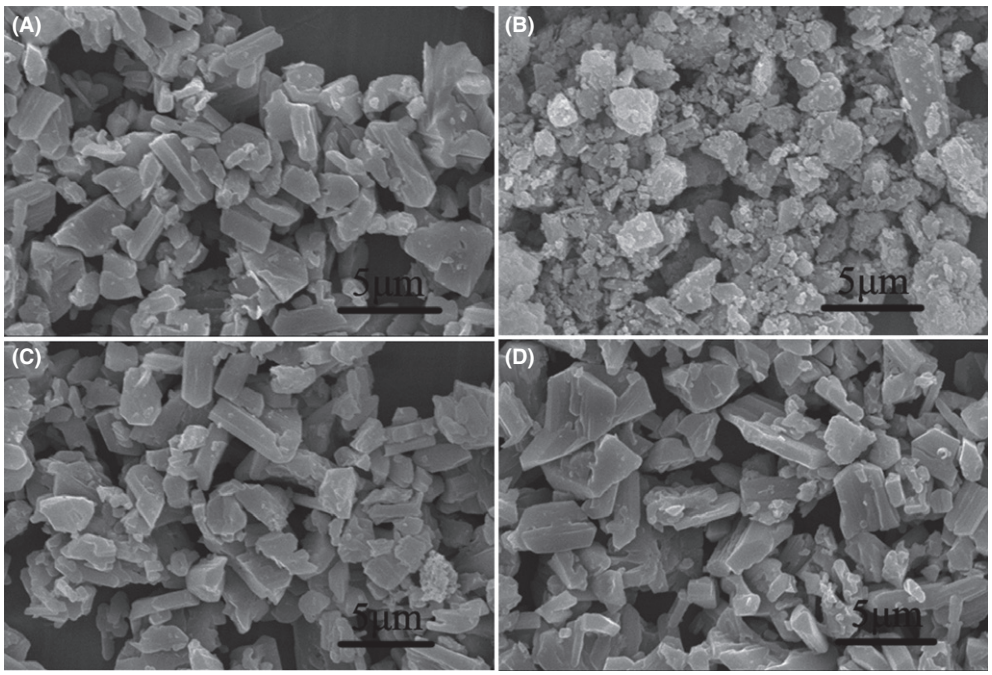

FIGURE 4 SEM images of SSN (A: as-prepared, B: treated at 150°C), and HB-SSN (C: as-prepared, D: treated at 150°C).

powders, which can be attributed to the newly formed phases. The formation of agglomerates of small particles is also observed and is more pronounced in the SSN powder.

Besides the improved hydrolysis resistance, the other advantage in HB-SSN is also brought out. The results of XANES measurements for SSN before and after the moisture tests at different temperatures and the comparison of the corresponding plots for SSN and HB-SSN after treatment at 150°C are shown in Figures 5(A) and (B), respectively. The two peaks at ca. 6977 and 6984 eV can be attributed to the divalent and trivalent oxidation states of Eu, respectively.[31] In SSN, the Eu^{3+} peak appears and becomes stronger with the increase in the temperature of heat treatment. A large number of Eu^{3+} ions seemingly formed in SSN treated at 150°C, whereas there is no evidence of Eu^{3+} peak in HB-SSN treated at the same temperature. These results suggest that HB-SSN shows improved oxidation resistance under high-pressure water steam.

The FT-IR spectra provide information about the structures of SSN and HB-SSN. According to Figure 6, the bands of (A) the Si–N–Si stretching vibrations (at ~472, ~926, and ~954 cm^{-1}),[32] (B) the molecular vibrations of H_2O (at ~1630 cm^{-1}),[33,34] and (C) due to Si–O–Si are seen in the spectra of both phosphors. However, in the spectrum of HB-SSN, there are two peaks at ~2960 and ~1260 cm^{-1} attributed to $–CH_3$ and $Si-CH_3$ groups, which are plausibly related to the hydrophobic behavior of HB-SSN and they improve the water resistance and provide remarkable stability of these phosphors in severe moisture conditions.[28,29,35]

The formation of a hydrophobic layer on the surface of the particles of HB-SSN, compared to SSN, was investigated with TEM and HRTEM analyses, as shown in Figure 7. A uniform amorphous layer with an average thickness of 8 nm tightly covered the surface of the HB-SSN particles, the inset electron-diffraction pattern of Figure 7(B) is from the $Sr_2Si_5N_8$ host. The element analysis with EDS (Figure 7D) shows that this layer is composed of Si, C, N, and O. According to these results, it is suggested that the formation of this hydrophobic layer starts with the hydrolysis of oxyethyl groups of TEOS due to the existence of surface-adsorbed water from ambient atmosphere,[36] followed by a condensation reaction between the hydrolyzed TEOS molecules and the surface hydroxyl or amido groups of SSN.[37] The formation of strong Si–O–Si and Si–N–Si bonds lead to the stronger adhesion of the hydrophobic layer. Finally, with the aid of DBTL, the hydrophobic layer forms through a polycondensation reaction between the terminal silanol groups of PDMS and the OH groups of hydrolyzed TEOS,[38] as illustrated in Figure 8.

On the other hand, Figures 7(C) and (D) suggest that an amorphous strontium silicon oxynitride layer forms on the as-prepared SSN particles.[39] This layer is formed by the oxidation and hydrolysis of the fresh surface of SSN when exposed to the air atmosphere for a long time,[40] which should occur along with the formation of defects. The

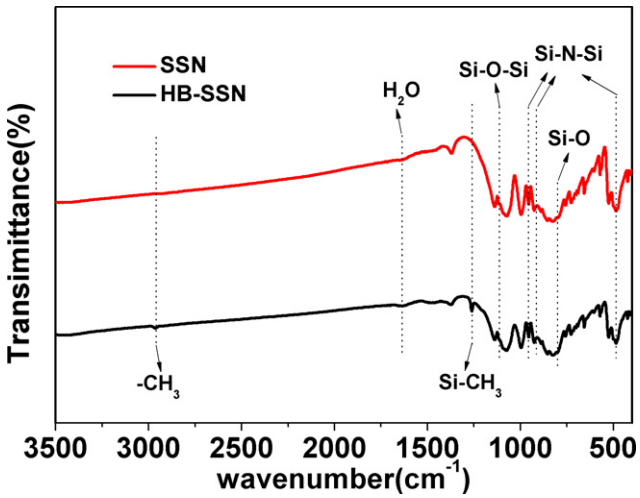

FIGURE 6 FT-IR spectra of SSN and HB-SSN [Color figure can be viewed at wileyonlinelibrary.com]

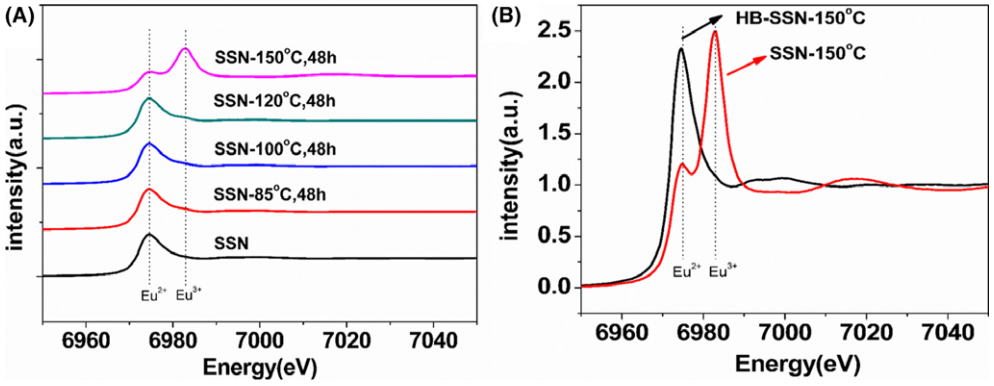

FIGURE 5 Normalized Eu L_{III}-edge XAFS of (A) SSN phosphors, as-prepared and after thermal treatment at different temperatures (for 48 hour), and (B) comparison of the corresponding plots for SSN and HB-SSN after thermal treatment at 150°C [Color figure can be viewed at wileyonlinelibrary.com]

transparent and thin surface layer formed in HB-SSN can effectively suppress the formation of this amorphous silicon oxynitride layer. This can explain why the as-produced HB-SSN has a slightly higher PL intensity than the as-produced SSN (Figure 2A). The decay times of SSN and HB-SSN were measured as 10.3 and 10.8 μsecond, respectively. This result suggests that the formation of the hydrophobic surface layer in HB-SSN suppresses the formation of defects in the surface.[41]

The results of thermal analysis (TGA and DTA curves), shown in Figure 9, provide information about the thermal stability of SSN and HB-SSN in air atmosphere. In HB-SSN, there is no weight loss up to 200°C, which suggests that the hydrophobic layer is stable enough for application in white LEDs. Meanwhile, there are no weight loss and weight gain up to about 700°C in the SSN. A slight weight loss above 200°C was recorded for HB-SSN, attributed to a release of gaseous species (e.g., NH_3, H_2, CH_4) and low molecular weight oligomers. An endothermic peak was recorded at ~550°C, which can probably be ascribed to the breaking of the interfacial bonding between the hydrophobic surface layer and the surface of the bulk SSN. The relative weight increase above 550°C should be a result of oxidation that occurred at the surface, while the oxidation of SSN starts at temperatures higher than 700°C.

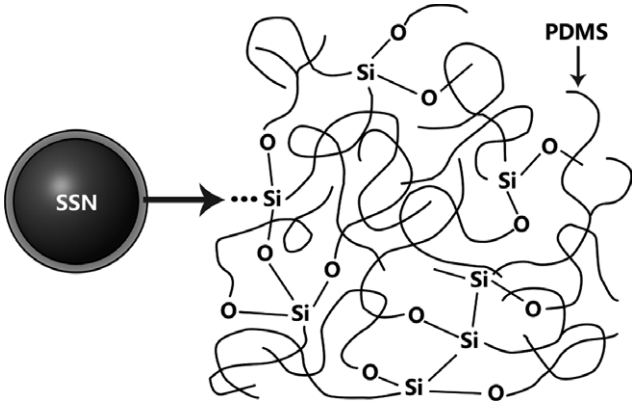

FIGURE 8 A schematic drawing of the structure on the surface of the SSN particle

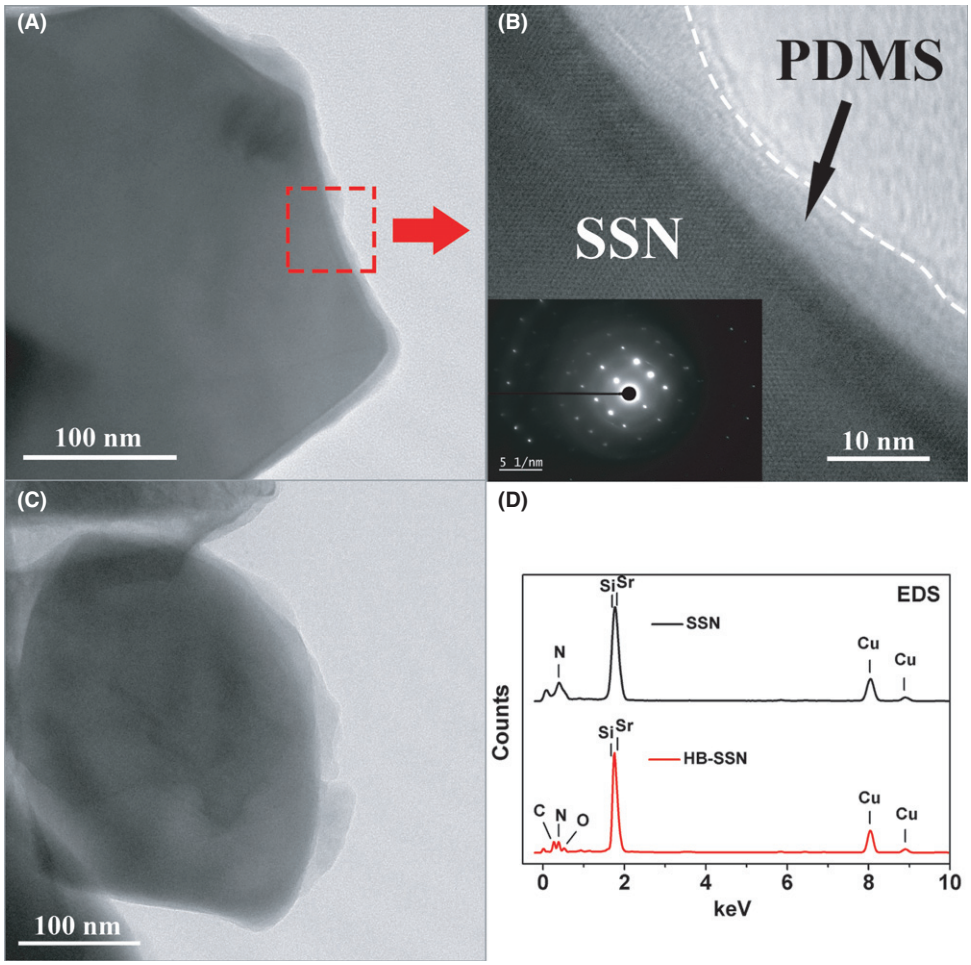

FIGURE 7 TEM (A) and HRTEM (B) images of HB-SSN, TEM image of SSN (C), and EDS spectra from the surface of SSN and HB-SSN particles (D) [Color figure can be viewed at wileyonlinelibrary.com]

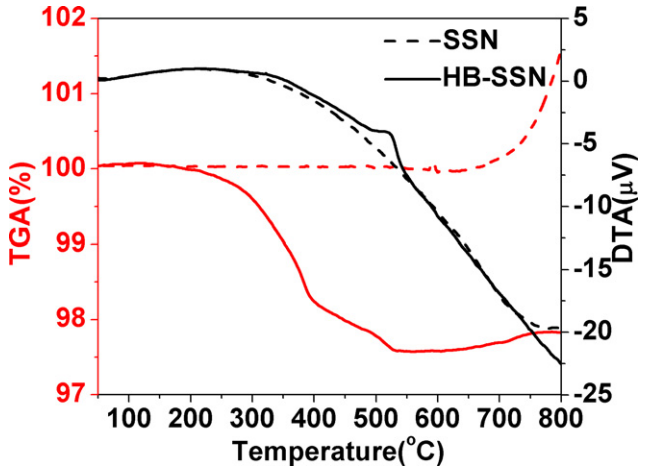

FIGURE 9 Thermal analysis (TGA and DTA curves) of SSN and HB-SSN in air atmosphere [Color figure can be viewed at wileyonlinelibrary.com]

This confirms that the hydrophobic layer in HB-SSN suppresses the formation of a silicon oxynitride layer.

4 | CONCLUSIONS

Significant luminescence degradation of SSN phosphors occurs at temperatures higher than 120°C under high-moisture conditions, due to the hydrolysis of the host and the oxidation of the activator (Eu^{2+}) via an oxidizing gas penetration mechanism. A hydrophobic modified surface layer was produced, which effectively improved the oxidation and hydrolysis resistance and the thermal stability of the produced phosphors under severe conditions of high-pressure water steam. The proposed method was developed to be potentially applied in other phosphors, such as silicate, (oxy)nitride, and aluminate phosphors, in order to provide stable phosphors in high humidity and temperature conditions.

ACKNOWLEDGMENTS

This research was supported by the National Natural Science Foundation of China (grant no. 51372238), the National Basic Research Program of China (973 Program, 2012CB922004), and the CNPC-CAS Strategic Cooperation Research Program (2015A-4812). The authors thank the BL14W1 beam line of Shanghai Synchrotron Radiation Facility for the XAFS measurements.

REFERENCES

1. Ju L-C, Xu X, Hao L-Y, Lin Y, Lee M-H. Modification of the coordination environment of Eu2+ in Sr2SiO4:Eu2+ phosphors to achieve full color emission. *J Mater Chem C*. 2015;3:1567–1575.
2. Xie R-J, Hirosaki N. Silicon-based oxynitride and nitride phosphors for white LEDs—A review. *Sci Technol Adv Mater*. 2007;8:588–600.
3. Song K-X, Zhang J-X, Liu Y-F, et al. Red-emitting phosphor Ba9Lu2-Si6O24:Ce3+, Mn2+ with enhanced energy transfer via self-charge compensation. *J Phys Chem C*. 2015;119:24558–24563.
4. Wang J, Zhang H-R, Liu Y-L, et al. Insights into luminescence quenching and detecting trap distribution in Ba2Si5N8:Eu2+ phosphor with comprehensive considerations of temperature-dependent luminescence behaviors. *J Mater Chem C*. 2015;3:9572–9579.
5. Yang X-F, Song H-L, Yang L-X, and Xu X.. Reaction mechanism of SrSi2O2N2:Eu2+ phosphor prepared by a direct silicon nitridation method. *J Am Ceram Soc*. 2011;94:164–171.
6. Li G-H, Chen J-J, Mao Z-Y, Song W-W, Sun T, Wang D-J. Atmospheric pressure preparation of red-emitting CaAlSiN3:Eu2+ phosphors with variable fluxes and their photoluminescence properties. *Ceram Int*. 2016;42:1756–1761.
7. Zhu Q-Q, Zhong L-X, Yang L-X, Xu X. Synthesis of the high performance YAG: Ce phosphor by a sol-gel method. *ECS J Solid State Sci Technol*. 2012;1:R119–R122.
8. Yeh C-W, Chen W-T, Liu R-S, et al. Origin of thermal degradation of Sr2−xSi5N8: Eux phosphors in air for light-emitting diodes. *J Am Chem Soc*. 2012;134:14108–14117.
9. Wang C-Y, Xie R-J, Li F, Xu X. Thermal degradation of the green-emitting SrSi2O2N2:Eu2+ phosphor for solid state lighting. *J Mater Chem C*. 2014;2:2735–2742.
10. Poelman D, Haecke JEV, Smet PF. Advances in sulfide phosphors for displays and lighting. *J Mater Sci: Mater Electron*. 2009;20:S134–S138.
11. Yu R-J, Wang J, Zhang M, et al. Luminescence properties of Ca1−xSrx (Ga1−yAly)2S4:Eu2+ and their potential application for white LEDs. *J Electrochem Soc*. 2008;155:J290–J292.
12. Zhu J, Wang L, Zhou T-L, et al. Moisture-induced degradation and its mechanism of (Sr, Ca)AlSiN3:Eu2+, a red-color-converter for solid state lighting. *J Mater Chem C*. 2015;3:3181–3188.
13. Brinkley SE, Pfaff N, Denault KA, et al. Robust thermal performance of Sr2Si5N8:Eu2+: An efficient red emitting phosphor for light emitting diode based white lighting. *Appl Phys Lett*. 2011;99:241106.
14. Kirakosyan AG, Jeon DY. Low-temperature synthesis of Sr2Si5N8:Eu2+ red-emitting phosphor by modified solid-state metathesis approach and its photoluminescent characteristics. *J Electrochem Soc*. 2012;159:J29–J33.
15. Nersisyan H, Won HI, Won CW. Highly effective synthesis and photoluminescence of Sr2Si5N8:Eu2+ red-emitting phosphor for LEDs. *Chem Commun*. 2011;47:11897–11899.
16. Suehiro T, Xie R-J, Hirosaki N. Gas-reduction−nitridation synthesis of CaAlSiN3:Eu2+ fine powder phosphors for solid-state lighting. *Ind Eng Chem Res*. 2014;53:2713–2717.
17. Kim Y, Kim J, Kang S. First-principles thermodynamic calculations and experimental investigation of Sr–Si–N–O system—synthesis of Sr2Si5N8: Eu phosphor. *J Mater Chem C*. 2013;1:69–78.
18. Zhang C-N, Uchikoshi T, Xie R-J, et al. Reduced thermal degradation of the red-emitting Sr2Si5N8:Eu2+ phosphor via thermal treatment in nitrogen. *J Mater Chem C*. 2015;3:7642–7651.
19. Hu Y-S, Zhuang W-D, He H-Q, et al. High temperature stability of Eu2+-activated nitride red phosphors. *J Rare Earths*. 2014;32:12–16.
20. Imai Y, Momoda R, Adachi Y, et al. Water-resistant surface-coating on europium-doped strontium aluminate nanoparticles. *J Electrochem Soc*. 2007;154:J77–J80.
21. Wu S, Zhang SF, Yang JZ. Highly water-resistant and organic miscible inorganic/polymer composite luminescent material. *Mater Lett*. 2009;63:1172–1174.
22. Deng S-Q, Xue Z-P, Yang Q, et al. Surface modification of MAl2O4: Eu2+, Dy3+ (M = Sr, Ca, Ba) phosphors to enhance water resistance by combustion method. *Appl Surf Sci*. 2013;282:315–319.
23. Wu S-L, Zhang S-F, Liu Y, Yang J-Z. The organic ligands coordinated long afterglow phosphor. *Mater Lett*. 2007;61:3185–3188.

24. Tang J-Y, Zhan C, Yang L-X, Hao L-Y, Xu X, Simeon A. Synthesis of h-BN encapsulated spherical core-shell structured SiO2@Sr2Si5N8:Eu2+ red phosphors. *Mater Chem Phys*. 2012;132:1089–1094.
25. Ionescu E, Kleebe H-J, Riedel R. Silicon-containing polymer-derived ceramic nanocomposites (PDC-NCs):preparative approaches and properties. *Chem Soc Rev*. 2012;41:5032–5052.
26. Colombo P, Mera G, Riedel R, Soraru GD. Polymer-derived ceramics: 40 years of research and innovation in advanced ceramics. *J Am Ceram Soc*. 2010;93:805–1837.
27. Flores A, Martos C, Sanchez-Cortes S, Rubio F, Rubio J, Oteo JL. Nanostructure and micromechanical properties of silica/silicon oxycarbide porous composites. *J Am Ceram Soc*. 2004;87:2093–2100.
28. Liu X, Li Y-L, Hou F. Fabrication of SiOC ceramic microparts and patterned structures from polysiloxanes via liquid cast and pyrolysis. *J Am Ceram Soc*. 2009;92:49–53.
29. Lu P, Huang Q, Liu B-D, Bando Y, Hsieh Y-L, Mukherjee AK. Macroporous silicon oxycarbide fibers with luffa-like superhydrophobic shells. *J Am Chem Soc*. 2009;131:10346–10347.
30. Yin LJ, Xu X, Yu W, et al. Synthesis of Eu2+-doped AlN phosphors by carbothermal reduction. *J Am Ceram Soc*. 2010;93:1702–1707.
31. Wang Y-F, Xu X, Yin L-J, Hao L-Y. High thermal stability and photoluminescence of Si–N-Codoped BaMgAl10O17:Eu2+ phosphors. *J Am Ceram Soc*. 2010;93:1534–1536.
32. Gomez-Serrano V, Pastor-Villegas J, Perez-Florindo A, Duran-Valle C, Valenzuela-Calahorro C. FT-IR study of rockrose and of char and activated carbon. *J Anal Appl Pyrolysis*. 1996;36:71–80.
33. Fleyfel F, Devlin JP. FT-IR spectra of carbon dioxide clusters. *J Phys Chem*. 1989;93:7292–7294.
34. Al-Abadleh HA, Grassian VH. FT-IR study of water adsorption on aluminum oxide surfaces. *Langmuir*. 2003;19:341–347.
35. Wang C-Y, Shen Z-X, Zheng J-Z. Thermal cure study of a low-k methyl silsesquioxane for intermetal dielectric application by FT-IR spectroscopy. *Appl Spectrosc*. 2000;54:209–213.
36. Blitz JP, Murthy RS, Leyden DE. Ammonia-catalyzed silylation reactions of Cab-O-Sil with methoxymethylsilanes. *J Am Ceram Soc*. 1987;109:7141–7145.
37. Liu G, Xiangli F, Wei W, Liu S, Jin W. Improved performance of PDMS/ceramic composite pervaporation membranes by ZSM-5 homogeneously dispersed in PDMS via a surface graft/coating approach. *Chem Eng J*. 2011;174:495–503.
38. Li KQ, Zeng XR, Li HQ, Lai XJ, Ye CX, Xie H. Study on the wetting behavior and theoretical models of polydimethylsiloxane/silica coating. *Appl Surf Sci* 2013; 279[x]: 458–463.
39. Ji WW, Ye SF, Lee M-H, et al. Influence of N-anion-doping on the production and the photoluminescence properties of γ-Ca2SiO4:Ce3+ phosphors and the β→γ phase transformation. *J Mater Chem C*. 2016;4:3313–3320.
40. Rahaman MN, Boiteux Y, DeJonghe LC. Surface characterization of silicon nitride and silicon carbide powders. *Am Ceram Soc Bull*; United States. 1986;65:1171–1176.
41. Yin LJ, Dong J, Wang Y, et al. Enhanced optical performance of BaMgAl10O17: Eu2 + phosphor by a novel method of carbon coating. *J Phys Chem C*. 2016;120:2355–2361.

How to cite this article: Zhang B, Wang J-W, Hao L-Y, Xu X, Agathopoulos S, Yin L-J, Wang C-M, (Bert) Hintzen HT. Highly stable red-emitting $Sr_2Si_5N_8:Eu^{2+}$ phosphor with a hydrophobic surface. *J Am Ceram Soc*. 2017;100:257–264. doi:10.1111/(ISSN)1551-2916.